

# Conductance enhancement due to the resonant tunneling into the subgap vortex core states in normal metal/superconductor ballistic junctions.

M. A. Silaev<sup>1</sup>

<sup>1</sup> Institute for Physics of Microstructures, Russian Academy of Sciences, 603950 Nizhny Novgorod, GSP-105, Russia

(Dated: February 1, 2008)

We investigate the low-energy quantum transport in ballistic normal metal-insulator - superconductor junction exposed to a magnetic field creating Abrikosov vortices in the superconducting region. Within the Bogoliubov- de Gennes theory we show that the presence of the subgap quasiparticle states localized within the vortex cores near the junction interface leads to the strong resonant enhancement of Andreev reflection probability, and the normal-to supercurrent conversion. The corresponding increase of charge conductance is determined by the distance from the vortex chain to the junction interface, which can be controlled by the applied magnetic field.

PACS numbers: 74.25.QP, 74.25.Fy, 73.40.Gk

## I. INTRODUCTION

Recently, the investigation of transport properties of normal metal- superconducting (N/S) hybrid structures has attracted a considerable interest. In the classical work by Blonder, Tinkham and Klapwijk<sup>1</sup> it was shown, that at the energies below the superconducting gap  $\Delta_0$  the charge transport can only be realized via the Andreev reflection at the N/S interface. This is a two-particle process in which the electrons with low energies  $\varepsilon < \Delta_0$  incident from the normal metal (N) are reflected at the N/S interface as holes traversing the backward trajectories (and vice versa). In accordance with the charge conservation law, at the superconducting region (S) the Cooper pairs are formed and the normal current converts into the supercurrent. For the perfectly transparent N/S interface the charge doubling due to Andreev reflection results in enhancement of the subgap conductance by a factor of two compared with the corresponding normal state conductance. Being the two-particle process Andreev reflection is strongly suppressed due to QP scattering at the layer of insulator separating the N and S regions. Indeed, in case of the small interfacial barrier transparency  $T \ll 1$ , the Andreev reflection probability, and therefore the conductance is proportional to  $T^2$  which is smaller by the factor  $T$  as compared to the single- electron case.

The phenomenon of subgap conductance suppression results in the remarkable dependence of transport properties of N/S structures on the spatial distribution and symmetry of the superconducting gap. For example, recently the charge current measurements were utilized for the direct observation of multi vortex structures in mesoscopic superconductors<sup>2</sup>. Mixed state of mesoscopic superconductors is formed by a small number of vortices and reveals a rich variety of exotic vortex configurations, such as vortex molecules and multiquantum giant vortices, realizing in such samples due to the quantum confinement of the Cooper pairs motion<sup>3</sup>. In Ref.2 the phase transitions between different vortex configurations were observed by the multiple-small-tunnel-junction method,

in which several small tunnel junctions were attached to the mesoscopic superconductor to simultaneously measure the charge transport at the different points of the sample. The measured transport characteristics were related to the local density of states (DOS), depending on the local supercurrent density and hence on the configuration of the vortex system. Generally, when there is a uniform supercurrent flowing at the superconductor, the excitation spectrum acquires a Doppler shift by the value  $\mathbf{v}_s \mathbf{p}_F$ , where  $\mathbf{v}_s$  is a superfluid velocity,  $\mathbf{p}_F$  is a Fermi momentum. In this case, the minimal excitation energy is given by  $E_{min} = \Delta_0 - \mathbf{v}_s \mathbf{p}_F$ . At large distances from the vortex core ( $r \gg \xi$ , where  $\xi$  is a coherence length) the Doppler shift model gives quite a good approximation of the quasiparticle (QP) spectrum with  $v_s = \hbar/2mr$  (see Ref.[4]). As long as the superfluid velocity is small compared to the critical value  $\Delta_0/p_F$ , the Doppler shift of the gap edge results in the reduction of the height and broadening of the superconducting DOS peak<sup>5</sup>. Close to the vortex core ( $r \sim \xi$ ) where  $v_s \sim \Delta_0/p_F$ , the gap edge  $E_{min}$  goes to zero. However, in this case the Doppler shift model does not hold: it completely misses one of the remarkable features of the vortex state: the presence of low-energy QP states localized within the vortex core. These vortex core states were found in the pioneering work by Caroli- de Gennes and Matricon (CdGM)<sup>6</sup> within the more rigorous approach based on the quasi-classical solution of Bogoliubov- de Gennes (BdG) equations. It was shown that QP states with energy lower than the bulk superconducting gap value  $\Delta_0$  are localized within the vortex core and have the discrete spectrum  $\varepsilon_\mu$  as a function of the quantized (half-integer) angular momentum  $\mu$ . This spectrum of the CdGM states varies from  $\Delta_0$  to  $-\Delta_0$  as  $\mu$  changes from  $-\infty$  to  $+\infty$ , crossing zero when  $\mu$  changes its sign. At small energies  $|\varepsilon| \ll \Delta_0$  the spectrum is given by  $\varepsilon_\mu \approx -\mu \epsilon_0$ , where  $k_F = p_F/\hbar$  and  $\epsilon_0 = \Delta_0/(k_F \xi)$ . For conventional superconductors, the interlevel spacing  $\epsilon_0$  is much less than the superconducting gap  $\Delta_0$  since  $(k_F \xi) \gg 1$ , therefore the CdGM spectrum can be considered continuous as a function of the impact parameter of quasiclassical trajectory

$b = -\mu/k_F$ . The presence of the QP states bounded in the vortex core was confirmed in scanning tunnel spectroscopy (STS) experiments by the observation of the zero-bias conductance peak at the vortex core<sup>7</sup>. The analogous effect of the zero-bias conductance enhancement due to the resonant tunneling into the midgap surface states was thoroughly studied in high temperature D-wave superconductors<sup>8</sup>.

The goal of our work is to develop a theory to calculate the zero-bias conductance of N/S junction in case when the external magnetic field generates vortices in the S region near the N/S interface. We consider the charge transport across the direction of applied magnetic field. The N and S regions are assumed to be separated by the interfacial barrier, suppressing the Andreev reflection and the electron transport. We predict the strong enhancement of the Andreev reflection due to the resonant tunneling of QP through the barrier into the CdGM states localized within the vortex cores. The essential physics of this effect is analogous to the one which takes place in double-barrier resonant tunneling diode<sup>9</sup>. The resonant tunneling in double-barrier quantum well structures occurs if the energy of incident QP wave coincides with the resonant energy, then the reflection probability is effectively suppressed due to the interference of the QP waves within the quantum well. In our case the quantum well is represented by the vortex core and the bounded low energy QP state consists of coupled electron and hole waves of almost the same amplitude. Therefore, if the incident electron has resonant energy, then the reflected electron wave is suppressed and the hole wave leaking from the vortex core contributes to the Andreev reflection probability. The important difference between our situation and the double-barrier diode case is that the spectrum of bound states is very dense with the characteristic interlevel spacing  $\epsilon_0 \sim \Delta_0/(k_F\xi)$  being much smaller than the bulk energy gap  $\Delta_0$ . At the same time, the broadening of this levels due to the finite barrier transparency can be estimated as  $\delta E \sim \Delta_0 T e^{-2a/\xi}$ , where  $T$  is the transparency of the interfacial barrier and the factor  $e^{-2a/\xi}$  is due to the exponential decay of subgap QP at the superconducting slab of the thickness  $a$ , which is in fact the distance from the vortex to the N/S interface,  $\xi$  is the superconducting coherence length. Hereafter in this paper we will neglect the discreteness of the bound energy levels assuming that  $T e^{-2a/\xi} \gg (k_F\xi)^{-1}$ . In fact this condition is not very restrictive since  $k_F\xi$  is large in many superconducting materials, for example  $k_F\xi \sim 3 \cdot 10^2$  in Nb and  $k_F\xi \sim 10^4$  in Al. Neglecting the discreteness of the spectrum of bounded QP states we can use the quasiclassical approximation of QP quantum mechanics (see e.g. Ref.10). Within such approximation QP move along linear trajectories, i.e. the straight lines along the direction of QP momentum  $\mathbf{n} = \mathbf{k}_F k_F^{-1} = (\cos \theta_p, \sin \theta_p)$ . Note, that for the N/S point contacts of atomic size in magnetic field it is necessary to take into account the non-quasiclassical divergence of the electron and hole trajectories<sup>11</sup>. In the present work we consider the trans-

port properties of wide N/S junction so that its transverse dimension  $L_y$  is much larger than the Fermi wave length  $L_y \gg \lambda_F = 2\pi/k_F$ , therefore the trajectory divergence can be neglected. Also we assume that  $L_y$  is much larger than the distance from the vortices to the N/S interface  $a$  and the characteristic intervortex distance  $L_v$ . The important point is that the total QP reflection probabilities can be found as a sum of individual vortex contributions. Indeed, the intervortex distance is much larger than the Fermi wavelength since  $L_v \geq \xi$  and  $k_F\xi \gg 1$ . Therefore, the quasiclassical trajectories (except those with  $\theta_p = \pm\pi/2$ ) can pass through not more than one vortex core. For some directions of QP momentum two resonant trajectories (i.e. passing through the vortex cores) are coupled by the normal reflection at the interfacial barrier. Assuming the specularly reflecting barrier this coupling occurs for the momentum angles at the narrow angle domains near  $\theta_p = \arctan(nL_v/2a)$ , where  $n$  is integer. The width of the resonant angle domains  $\delta\theta \sim T e^{-2a/\xi} \ll \pi$  is determined by the width of the resonant vortex core levels. Therefore, the contribution of such trajectories to the amplitude of the reflected QP waves is negligible. Then, evaluating the amplitude of the QP wave we can separate the resonant trajectories coupled with bounded QP states localized within the different vortex cores. Since different trajectories do not interfere with each other, the resulting reflection probabilities and the conductance can be found as a sum of contributions from individual vortices.

The dimensionless conductance (further we will measure it in terms of the conductance quantum  $e^2/\pi\hbar$ ) induced by a single vortex at zero temperature can be estimated as follows:  $G_v \sim N_r e^{-2a/\xi} T$ . Here  $N_r \sim k_F\xi$  is the number of transverse modes of the N/S junction which effectively interact with the QP states bounded within the vortex core ( $\xi$  is the characteristic transverse size of the vortex core). The factor  $e^{-2a/\xi} T$  is the one-particle tunneling probability through the barrier consisting of the insulating layer at the N/S interface and the superconducting slab of the thickness  $a$ . The total vortex-induced conductance is the sum of the individual vortex contributions  $G_{vt} = n_v G_v$ , where  $n_v = L_y/L_v$  is the total number of vortices near the N/S interface,  $L_v$  is the intervortex spacing and  $L_y$  is the transverse size of the junction. The resonant mechanism of Andreev reflection exists along with the usual non-resonant scheme involving the two-particle tunneling through the interfacial barrier with the probability  $T^2$ . The corresponding zero-bias conductance can be estimated as  $G_0 \sim N_0 T^2$ , where  $N_0 = k_F L_y/\pi$  is the total number of transverse modes in N/S junction. Therefore, the total conductance of the N/S junction in magnetic field can be evaluated as follows:

$$G = \alpha N_0 T^2 + n_v \beta N_r e^{-2a/\xi} T, \quad (1)$$

where the coefficients  $\alpha, \beta \sim 1$ . Then, for the strong barrier  $T \ll 1$ , the conductance induced by the vortex chain with spacing  $L_v$  becomes dominant at  $a < a_c$ , where the

threshold distance  $a_c \sim (\xi/2) \ln(\xi/T L_v)$  can be much larger than the vortex core size and the coherence length.

The parameters of the vortex lattice can be estimated as follows:  $a, L_v \sim \sqrt{\phi_0/B}$ , where  $B$  is the average magnetic field of the superconducting sample and  $\phi_0 = \pi \hbar c/e$  is the flux quantum. Then, the magnetic field dependence of the vortex-induced second term in Eq.(1) conductance is given by:

$$G_{vt} \sim N_0 \sqrt{\frac{B}{H_{c2}}} e^{-2\sqrt{H_{c2}/B}} T, \quad (2)$$

where  $H_{c2} \sim \phi_0/\xi^2$  is the upper critical magnetic field of the superconductor. Note, that at zero magnetic field  $B = 0$  the conductance is  $G \sim N_0 T^2$  and at  $B = H_{c2}$  the conductance is much larger:  $G \sim N_0 T$ . Therefore, we suggest that if the surface barrier is high  $T \gg 1$ , it should be possible to observe in experiment the field-induced increase of the conductance according to the Eq.(2).

In the present work we do not take into account the subgap QP states which exists near the surface of superconductor due to the Meissner screening of external magnetic field<sup>12</sup>. Such QP levels lie higher at the energy scale than the CdGM states if the density of supercurrent near the surface is less than the critical value. Therefore, as long as the zero-bias conductance is considered the influence of the surface QP states can be neglected.

The paper is organized as follows. In Sec. II a description of the model and the basic equations are given. In Sec. III we solve the scattering problem to find the Andreev and normal reflection probabilities. Sec. IV is devoted to the conductance calculation and Sec.V to the discussion of obtained results. Finally, conclusions are given in Sec. VI.

## II. MODEL AND BASIC EQUATIONS

Shown on the Fig.(1) is the scheme of the N/S junction with vortex lines in the S region parallel to the N/S interface. For the sake of simplicity we assume that there is only one quantized QP mode in  $z$  direction and take into account only the QP motion in  $xy$  plane, perpendicular to the vortex lines.

Considering one vortex from the array, the coordinate system is chosen so that the  $z$  axis coincides with the vortex line and the origin at the  $xy$  plane coincides with vortex phase singularity point. Neglecting the suppression of the superconductivity near the N/S interface due to the proximity effect we assume that at  $x > -a$  (superconducting region) the order parameter can be taken as follows:

$$\Delta(\mathbf{r}) = \Delta_0 D_v(\mathbf{r}) e^{i\Phi(\mathbf{r})}, \quad (3)$$

Here  $\Delta_0$  is the gap value far from the vortex core,  $D_v(\mathbf{r})$  and  $\Phi(\mathbf{r})$  are the dimensionless profile and the phase of the order parameter. The particular form of  $D_v(\mathbf{r})$  is not essential for our consideration, therefore it can be chosen

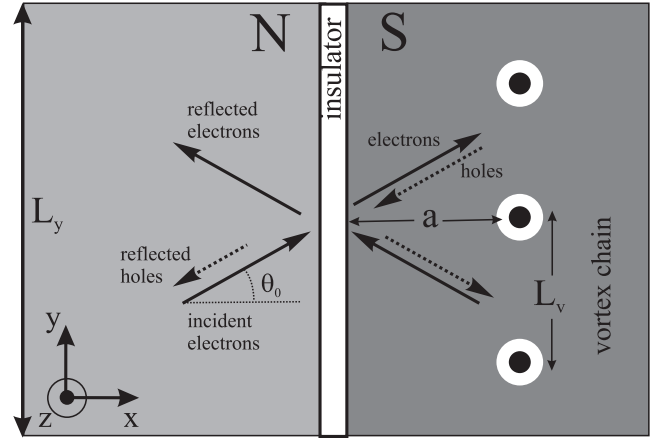


FIG. 1: Geometry of N/S junction and sketch of QP trajectories. The width of the junction is  $L_y$ . External magnetic field directed along  $z$  axis introduces vortices in superconductor. The distance from the first vortex chain to the N/S interface is  $a$ , and the intervortex spacing is  $L_v$ . The electrons are injected with the incident angle  $\theta_0$  and experience Andreev and normal reflection at the N/S interface.

similar to the model profile of the isolated vortex core<sup>13</sup>:  $D_v(\mathbf{r}) = r/\sqrt{r^2 + \xi^2}$ , where  $\xi$  is the coherence length. The phase distribution  $\Phi(\mathbf{r})$  consists of a singular part  $\Phi_v(\mathbf{r}) = \arg(\mathbf{r})$  and a regular part  $\Phi_r(\mathbf{r})$ , determined by the particular metastable vortex lattice configuration realizing near the boundary.

In principle, the method developed in the present paper is applicable to the arbitrary order parameter phase distribution corresponding to the metastable vortex configuration. At first, we solve a generic problem of the influence of a single vortex near the N/S surface on the zero-bias conductance of the junction. The vortex stability condition given by the London model, requires vanishing regular part of the superfluid velocity at the vortex position:  $(\nabla \Phi_r - (2\pi/\phi_0)\mathbf{A})(\mathbf{r} = 0) = 0$ , where  $\mathbf{A}$  is the vector potential. On the microscopic level, this condition is necessary for the existence of the CdGM QP states forming the vortex phase singularity<sup>14,15</sup>. The next step is the summation of the individual vortex contributions to the conductance which add independently. The particular vortex configuration near the boundary depends on many factors, such as the random pinning potential, geometry of the superconducting sample, magnetization history, etc. To estimate the dependence of the conductance on the magnetic field we consider the model situation assuming that the vortices near the boundary of superconductor sit periodically on chain with an intervortex spacing  $L_v$  at a distance  $a$  from the N/S interface. We take  $a$  and  $L_v$  as external parameters of the order  $a, L_v \sim \sqrt{\phi_0/B}$ , where  $B$  is the average magnetic field of the superconducting sample. The influence of the next vortex chains on the conductance can be neglected due to the rapid decay of the QP tunneling probability with

the growing distance from vortices to the N/S interface.

The expression for the dimensionless zero-bias conductance of the N/S junction can be written as follows (see Ref.1):

$$G = \frac{N_0}{2} \int_{-\pi/2}^{\pi/2} (1 - R_n(\theta_0) + R_a(\theta_0)) \cos \theta_0 d\theta_0, \quad (4)$$

where  $R_n(\theta_0)$  and  $R_a(\theta_0)$  are the probabilities of normal and Andreev reflection respectively,  $\theta_0$  is the incident angle:  $\mathbf{k}_F = k_F(\cos \theta_0, \sin \theta_0)$ . The total number of propagating modes  $N$  is determined by the channel width:  $N_0 = k_F L_y / \pi$ . The problem of QP scattering at the N/S interface is formulated within the BdG theory. The equation for the electron and hole waves coupled by the superconducting gap  $\Delta(\mathbf{r})$  reads as follows:

$$\begin{pmatrix} \hat{H}_0(\mathbf{r}) & \Delta(\mathbf{r}) \\ \Delta^*(\mathbf{r}) & -\hat{H}_0(\mathbf{r}) \end{pmatrix} \hat{\Psi}(\mathbf{r}) = E \hat{\Psi}(\mathbf{r}), \quad (5)$$

Here

$$\hat{H}_0(\mathbf{r}) = \frac{1}{2m} \left( \hat{\mathbf{p}} - \frac{e}{c} \mathbf{A} \right)^2 - E_F + V(x)$$

with  $\hat{\mathbf{p}} = -i\hbar\nabla$ ,  $\hat{\Psi}(\mathbf{r}) = (u(\mathbf{r}), v(\mathbf{r}))$ . The interfacial barrier separating the N and S regions is modeled by the repulsive delta potential  $V(x) = H\delta(x)$ , parameterized by the dimensionless barrier strength  $Z = H/\hbar V_F$ . The boundary conditions at the N/S interface are:

$$[\hat{\Psi}(-a)] = 0, \quad (6)$$

$$[\partial_x \hat{\Psi}(-a)] = (2k_F Z) \hat{\Psi}(-a), \quad (7)$$

where  $[f(x)] = f(x+0) - f(x-0)$ .

To overcome the complexity of the scattering problem coming from the broken spatial invariance of the superconducting gap, we treat the Eq.(5) within quasiclassical approximation. Generally, the quasiclassical form of the wave function can be constructed as follows:  $\hat{\Psi}(\mathbf{r}) = e^{i\mathbf{k}_F \cdot \mathbf{r}} \hat{f}(\mathbf{r})$ , where  $\hat{f}(\mathbf{r}) = (U(\mathbf{r}), V(\mathbf{r}))$  is a slow varying envelope function. Then the system (5) reduces to the system of the first-order quasiclassical equations along the linear trajectories defined by the direction of the QP momentum  $\mathbf{n} = \mathbf{k}_F k_F^{-1} = (\cos \theta_p, \sin \theta_p)$ . Each trajectory is specified by the angle  $\theta_p$  and the impact parameter  $b = r \sin(\theta - \theta_p)$ , where  $\theta$  is the polar angle:  $\mathbf{r} = -r(\cos \theta, \sin \theta)$ . Introducing the coordinate along trajectory  $s = (\mathbf{n} \cdot \mathbf{r}) = -r \cos(\theta_p - \theta)$  we arrive at the following form of the quasiclassical equation:  $\hat{H} \hat{f} = \epsilon \hat{f}$ , with the hamiltonian:

$$\hat{H} = -i\xi \hat{\sigma}_z \partial_s + F + D_v (\hat{\sigma}_x \cos \Phi - \hat{\sigma}_y \sin \Phi), \quad (8)$$

where  $\epsilon = E/\Delta_0$ ,  $\xi = \hbar V_F/\Delta_0$  is the coherence length,  $D_v(\mathbf{r})$  and  $\Phi(\mathbf{r})$  are the dimensionless magnitude and phase of the order parameter and  $F(\mathbf{r}) = (\pi\xi/\phi_0)\mathbf{n} \cdot \mathbf{A}$ .

Considering the zero-bias problem we will have to analyze only the zero-energy excitations with  $\epsilon = 0$ . Within the normal metal region at  $x < -a$ , neglecting the influence of magnetic field on the QP motion, the quasiclassical equation (8) becomes trivial:  $\partial_s \hat{f}(s, b) = 0$ . It means that the envelope function is constant along the trajectories.

Obviously, this is not the case at the superconducting region  $x > -a$ , where the electron and hole waves are coupled. Note that for the wave functions at the S region corresponding to the zero energy the following representation can be used<sup>10</sup>:  $\hat{f} = e^\zeta (e^{i(\eta+\Phi)/2}, e^{-i(\eta+\Phi)/2})$ , where  $\zeta = \zeta(s, b)$  and  $\eta = \eta(s, b)$  are real-valued functions. Then, the quasiclassical equation (8) can be written as follows:

$$\xi \partial_s \zeta + 2D_v \cos \eta + \epsilon_d = 0, \quad (9)$$

$$\xi \partial_s \zeta + 2D_v \sin \eta = 0. \quad (10)$$

where  $\epsilon_d(\mathbf{r}) = \hbar \mathbf{k}_F \mathbf{v}_s / \Delta_0$  is the dimensionless Doppler shift energy. For the wave functions  $\hat{f}_\pm$  decaying at the different ends of the trajectory  $\hat{f}_\pm(s = \pm\infty) = 0$  from Eq.(10) we obtain:

$$\eta_\pm(s = \pm\infty) = \pm\pi/2. \quad (11)$$

As we will see below, the main contribution to the enhanced Andreev reflection probability comes from the trajectories with small impact parameters  $|b| \ll \xi$ , passing through the vortex core. For such trajectories neglecting the nonsingular part of the superfluid velocity near the vortex core the analytical solution of Eq.(9) can be obtained following the results of Ref.16:

$$\tan \eta_\pm = 0.5 \left( A_\pm^{-1} e^{-2K(s)} - A_\pm e^{2K(s)} \right), \quad (12)$$

$A_\pm = \gamma(b)(\text{sgn}(s) \mp 1)$ , where  $\gamma(b) = -\omega b$ ,

$$K(s) = \frac{1}{\xi} \int_0^s D_v(s') ds' = \sqrt{(s/\xi)^2 + 1} - 1,$$

$$\omega = \frac{1}{\xi} \int_0^\infty \frac{D_v(s)}{s} e^{-2K(s)} ds.$$

### III. SCATTERING PROBLEM: NORMAL AND ANDREEV REFLECTION PROBABILITIES

The boundary conditions (6,7) determine the specularly reflecting N/S interface, coupling the waves with

wave vectors  $\mathbf{k}_F = k_F(\cos\theta_0, \sin\theta_0)$ , and  $\mathbf{k}'_F = k_F(\cos(\pi - \theta_0), \sin(\pi - \theta_0))$ . Therefore if the incident electron wave is  $u_i = e^{i\mathbf{k}_F \cdot \mathbf{r}}$ , then reflected electron  $u_r$  and hole  $v_r$  waves will have the form

$$u_r = U_r e^{i\mathbf{k}'_F \cdot \mathbf{r}}, \quad v_r = V_r e^{i\mathbf{k}_F \cdot \mathbf{r}},$$

where and  $U_r(b, s)$  and  $V_r(s, b)$  are the envelope functions. Each point  $(-a, y)$  at the N/S interface lies on the intersection of two quasiclassical trajectories, characterized by the angles  $\theta_p = \theta_0$  and  $\theta_p = \pi - \theta_0$ . From the simple trigonometry it is easy to see that the impact parameters of these trajectories are  $b_+ = -a \sin(\theta_0 - \theta)/\cos\theta$  and  $b_- = -a \sin(\theta_0 + \theta)/\cos\theta$  correspondingly, where  $\theta = -\arctan(y/a)$  is the polar angle. The coordinate of the intersection point is  $s_+ = -a \cos(\theta - \theta_0)/\cos\theta$  and  $s_- = a \cos(\theta + \theta_0)/\cos\theta$  for the trajectories characterized by the angles  $\theta_p = \theta_0$  and  $\theta_p = \pi - \theta_0$  correspondingly. Then, the reflection probabilities are given by:

$$R_n(\theta_0) = \frac{a}{L_y} \int_{-\alpha}^{\alpha} |U_r(\theta, \theta_0)|^2 (\cos\theta)^{-2} d\theta \quad (13)$$

$$R_a(\theta_0) = \frac{a}{L_y} \int_{-\alpha}^{\alpha} |V_r(\theta, \theta_0)|^2 (\cos\theta)^{-2} d\theta, \quad (14)$$

where the integration is done over the N/S interface,  $\alpha = \arctan(L_y/2a)$ ,  $U_r(\theta, \theta_0) = U_r(b_-, s_-)$  and  $V_r(\theta, \theta_0) = V_r(b_+, s_+)$ .

Following the usual procedure, to find the reflected wave amplitudes  $U_r(\theta, \theta_0)$  and  $V_r(\theta, \theta_0)$  one needs to match the N and S regions solutions at the N/S interface. For the envelope functions the boundary conditions (6,7) yield:

$$1 + U_r = e^{i\eta_+/2} C^+ + e^{i\eta_-/2} C^-,$$

$$V_r = e^{-i\eta_+/2} C^+ + e^{-i\eta_-/2} C^-,$$

$$(1 - U_r) + 2iZ(1 + U_r) = e^{i\eta_+/2} C^+ - e^{i\eta_-/2} C^-,$$

$$V_r(1 + 2iZ) = e^{-i\eta_+/2} C^+ - e^{-i\eta_-/2} C^-,$$

$C^+, C^-$  are arbitrary constants and  $\eta_{\pm} = \eta_{\pm}(s_{\pm}, b_{\pm})$ , where  $\eta_{\pm}(s, b)$  are the solutions of Eq.(9) with boundary conditions (11) along the trajectories with  $\theta_p = \theta_0$  and  $\theta_p = \pi - \theta_0$  for the upper and lower signs correspondingly.

Solving this system we obtain:

$$U_r(\theta, \theta_0) = -\frac{(1 - e^{i\chi})(\tilde{Z}^2 - i\tilde{Z})}{1 + \tilde{Z}^2(1 - e^{i\chi})}, \quad (15)$$

$$V_r(\theta, \theta_0) = \frac{e^{-i\eta_+}}{1 + \tilde{Z}^2(1 - e^{i\chi})}, \quad (16)$$

where  $\chi(\theta, \theta_0) = \eta_- - \eta_+$  and  $\tilde{Z} = Z/\cos\theta_0$ .

Note, that for the small impact parameters  $|b_{\pm}| \ll \xi$  the factors  $e^{i\eta_{\pm}}$  can be obtained analytically with the help of Eq.(12) as follows:

$$e^{i\eta_+} = i \frac{J - i(\theta - \theta_0)}{J + i(\theta - \theta_0)}, \quad (17)$$

$$e^{i\eta_-} = -i \frac{J - i(\theta + \theta_0)}{J + i(\theta + \theta_0)}, \quad (18)$$

where  $J = e^{-2K(a/\cos\theta)} \cos\theta/(2\omega a)$ . For the small angles  $|\theta|, |\theta_0| \ll \xi/a$  the equations (17) and (18) are valid simultaneously yielding:

$$e^{i\chi} = -\frac{J^2 + \theta^2 - \theta_0^2 - 2i\theta_0 J}{J^2 + \theta^2 - \theta_0^2 + 2i\theta_0 J}. \quad (19)$$

#### IV. VORTEX-INDUCED ZERO-BIAS CONDUCTANCE

Now, using the expressions (15, 16) for the amplitudes of reflected waves and reflection probabilities (13, 14) it is possible to find the zero-bias conductance. Introducing the function  $g(\theta, \theta_0) = 1 - |U_r(\theta, \theta_0)|^2 + |V_r(\theta, \theta_0)|^2$  the expression for the dimensionless conductance (4) reads as follows:

$$G = \frac{k_F a}{2\pi} \int_{-\alpha}^{\alpha} (\cos\theta)^{-2} d\theta \int_{-\pi/2}^{\pi/2} g(\theta, \theta_0) \cos\theta_0 d\theta_0, \quad (20)$$

where  $\alpha = \arctan(L_y/2a)$ . It is convenient also to introduce here a local conductivity, i.e. the conductance per unit length of the N/S surface:

$$\sigma(\theta) = \frac{k_F}{2\pi} \int_{-\pi/2}^{\pi/2} g(\theta, \theta_0) \cos\theta_0 d\theta_0.$$

Employing Eqs.(15,16) we obtain:

$$g(\theta, \theta_0) = \frac{2}{(\tilde{Z}^4 + \tilde{Z}^2)|1 - e^{i\chi}|^2 + 1}. \quad (21)$$

If the applied magnetic field is zero and the superconductor is homogeneous  $\chi = \pi$ , we obtain  $g(\theta, \theta_0) = g_0(\theta_0)$ , where  $g_0(\theta_0) = (1/2)(\tilde{Z}^2 + 1/2)^{-2}$ . Then, the vortex-induced part of the conductivity is given by

$$\sigma_v(\theta) = \frac{k_F}{2\pi} \int_{-\pi/2}^{\pi/2} g_v(\theta, \theta_0) \cos\theta_0 d\theta_0,$$

where  $g_v = g - g_0$ :

$$g_v = \frac{(\tilde{Z}^4 + \tilde{Z}^2)(4 - |1 - e^{i\chi}|^2)}{2(\tilde{Z}^2 + 1/2)^2 ((\tilde{Z}^4 + \tilde{Z}^2)|1 - e^{i\chi}|^2 + 1)}.$$

To start the analysis of Eq.(21) let's note that for the low surface barrier  $\tilde{Z} \rightarrow 0$  we get  $g_v(\theta, \theta_0) = 0$ . In this case all the incident QP undergo Andreev reflection and the zero-bias conductance is the same as in case of homogeneous superconductor:  $G = 2N_0$ . As the barrier becomes higher, the Andreev reflection is suppressed and the conductance is reduced.

The function  $g_v(\theta, \theta_0)$  reaches its maximum

$$g_{vm} = 2 \frac{\tilde{Z}^4 + \tilde{Z}^2}{(\tilde{Z}^2 + 1/2)^2}$$

if  $|1 - e^{i\chi}| = 0$ . In fact this condition determines the resonant trajectories, corresponding to the zero-energy vortex core states modified by the normal reflection from the interfacial barrier. The resonant trajectories should pass through the vortex core therefore the function  $g_v(\theta, \theta_0)$  has a sharp peak at  $\theta_0 \approx \pm\theta$ . The width of this peak is determined by the barrier strength and the distance from the vortex to the surface. For the small angles  $|\theta|, |\theta_0| \ll \xi/a$  with the help of Eq.(19) we obtain:

$$g_v(\theta_0, \theta) = \frac{g_{vm} J_0^2 \theta_0^2}{(\tilde{Z}^2 + 1/2)^2 (\theta_0^2 - \theta^2 - J_0^2)^2 + J_0^2 \theta_0^2}, \quad (22)$$

where  $J_0 = e^{-2K(a)} / (2\omega a) \sim (\xi/a)e^{-2a/\xi}$ , which is a small parameter since  $J \ll 1$  for  $a \geq \xi$ . The maximum of  $g_v(\theta, \theta_0)$  determined by Eq.(22) lies at  $\theta_0^2 = \theta^2 + J_0^2$ .

Employing Eq.(22) it is easy to compute the vortex-induced part of the conductivity  $\sigma_v(\theta)$  at the small angle domain  $|\theta| \ll \xi/a$ . The main contribution to integral over  $\theta_0$  comes from the small vicinity of the point  $\theta_0 = \theta$ . Then with good accuracy we obtain:  $\sigma_v = \sigma_{v0}$ , where

$$\sigma_{v0} = k_F J_0 \frac{Z^4 + Z^2}{(Z^2 + 1/2)^3}. \quad (23)$$

At larger angles the function  $\sigma_v(\theta)$  can be evaluated only numerically. Numerical calculation described below shows that  $\sigma_v(\theta)$  is maximal at  $\theta = 0$  and steadily decreases to zero as  $|\theta| \rightarrow \pi/2$ . (see inset on Fig.2). Then, the resulting conductance induced by a single vortex  $G_v = a \int_{-\alpha}^{\alpha} (\cos \theta)^{-2} \sigma_v(\theta) d\theta$  is given by:

$$G_v = \beta(k_F \xi) e^{-2K(a)} \frac{Z^4 + Z^2}{(Z^2 + 1/2)^3}, \quad (24)$$

where  $\beta = (2\omega\xi)^{-1} \int_{-\alpha}^{\alpha} (\cos \theta)^{-2} \sigma_v(\theta) / \sigma_{v0} d\theta \sim 1$ .

To evaluate the conductance rigorously, we find the factor  $e^{i\chi}$  in Eq.(21) and then the reflection probabilities solving numerically Eq.(9) with boundary conditions (11). We assume that the regular part of the phase distribution is  $\Phi_r(\mathbf{r}) = -\text{arg}(\mathbf{r} - \mathbf{r}_{av})$  corresponding to the image vortex situated at the point  $\mathbf{r}_{av} = (-2a, 0, 0)$  behind the N/S interface. The vector potential is chosen as  $\mathbf{A} = B [\mathbf{z}_0 \times (\mathbf{r} - \mathbf{r}_0)] / 2$ , where  $\mathbf{r}_0 = (-a, 0, 0)$  is the point at the boundary between the vortex and the image vortex, and  $\mathbf{z}_0$  is the unit vector along the  $z$  axis.

Within such model the condition of vanishing current through the N/S interface ( $\partial_x \Phi - (2\pi/\phi_0)\mathbf{A}_x = 0$ ) is satisfied automatically, and the vortex stability is achieved by setting  $a = \sqrt{\phi_0/B}$ . The numerical plot of the function  $\sigma_v(\theta)/\sigma_{v0}$  at different distances  $a$  from the vortex to the interface is presented on the inset at Fig.(2). The maximum value  $\sigma_v(\theta = 0)$  with good accuracy coincides with the analytical estimation given by (23). The coefficient  $\beta$  in Eq.(24) is found to be nearly constant as a function of  $a$ : it decreases slightly from  $\beta \simeq 0.6$  at  $a = 2\xi$  to  $\beta \simeq 0.4$  at  $a = 5\xi$ . On the Fig.(2) for the various magnitude of barrier strength we plot the ratio  $\bar{\sigma}_v/\sigma_0$  of the average vortex-induced conductivity  $\bar{\sigma}_v = G_v/\xi$  to the conductivity of the N/S junction in the absence of vortices given by:

$$\sigma_0 = \frac{k_F}{2\pi} \int_{-\pi/2}^{\pi/2} g_0(\theta, \theta_0) \cos \theta_0 d\theta_0.$$

## V. DISCUSSION

Considering the strong barriers  $Z \gg 1$  Eq.(24) can be written as  $G_v = \beta(k_F \xi) e^{-2K(a)} T$ , where we introduced the barrier transparency  $T = (1 + Z^2)^{-1} \approx Z^{-2}$ . A simple understanding of this result can be obtained within the framework of the tunneling hamiltonian approach<sup>17</sup>. The conventional expression for the tunneling conductivity of the N/S junction at zero temperature reads:

$$\sigma = \sigma_n \nu / \nu_0, \quad (25)$$

where  $\nu$  is a local superconducting DOS at the Fermi level and  $\sigma_n$  is a normal state tunneling conductivity. For the S-wave superconductor the transformation of vortex core states near the surface can be neglected at first approximation<sup>18</sup>. Then the local DOS near the surface at the Fermi level is determined by the density of vortex core states  $\nu_v(\mathbf{r})$  given by<sup>19,20</sup>:

$$\nu_v(\mathbf{r}) = \frac{1}{2\pi} \int_0^{2\pi} |\hat{f}(\mathbf{r}, \theta_p)|^2 \delta(\epsilon_0 k_F r \sin(\theta - \theta_p)) d\theta_p, \quad (26)$$

where  $\hat{f}(\mathbf{r}, \theta_p)$  is the envelope of the QP wave function. For the CdGM wave functions  $|\hat{f}(\mathbf{r}, \theta_p)|^2 \sim e^{-2K(r)} k_F / \xi$ , then  $\nu_v(\mathbf{r}) \sim \nu_0(\xi/r) e^{-2K(r)}$ , where  $\nu_0 = m/\hbar^2$  is the two-dimensional DOS at the normal metal. Substituting  $\nu = \nu_v(r = a/\cos\theta)$  and  $\sigma_n \sim Tk_F$  we obtain the conductivity:  $\sigma \sim k_F T J(\theta)$ , which coincides to the order of magnitude with expression (23) if  $Z \gg 1$  and  $|\theta| \ll 1$ . Integrating  $\sigma(\theta)$  over the N/S interface we arrive at expression (24) for the conductance with factor  $\beta$  given by:  $\beta \sim \int_{-\alpha}^{\alpha} \exp(2K(a) - 2K(a/\cos\theta)) (\cos \theta)^{-1} d\theta$ . Note, that although yielding the qualitatively right answer for the vortex-induced conductance, the tunneling hamiltonian approach drops out the contribution from the non-resonant Andreev reflection with the probability of the order  $T^2$ . As we will see below, the contributions

of the resonant and non-resonant Andreev reflections can be comparable even when the surface barrier is rather strong. Certainly, the tunneling hamiltonian approach fails to provide the answer if the barrier strength is not very high, when the influence of vortices on the conductance is reduced and the non-resonant Andreev reflection prevails. On the Fig.3a we show in logarithmic scale the vortex induced conductivity  $\bar{\sigma}_v$  as a function of the barrier strength  $Z$  for the several values of the distance  $a$ . At small values of  $Z$  the function  $\bar{\sigma}_v(Z)$  grows  $\bar{\sigma}_v \sim Z^2$  in accordance with the estimation (23). At larger values of the barrier strength  $Z \gg 1$  the behaviour of  $\bar{\sigma}_v(Z)$  changes to  $\bar{\sigma}_v \sim Z^{-2}$ . But at the same time the conductivity without vortices at  $Z \gg 1$  behaves as  $\sigma_0 \sim Z^{-4}$ . Therefore, the ratio  $\bar{\sigma}_v/\sigma_0$  is monotonically growing as a function of the barrier strength  $Z$  proportional to  $Z^2$  (see Fig.3b).

Let's have a look at the expression for the total conductance of the N/S junction, which has quite a simple form if  $Z \gg 1$ . Neglecting edge effects and summing up the individual vortex contributions we obtain:

$$G = (8/15)N_0T^2 + n_v\beta(k_F\xi)e^{-2K(a)}T, \quad (27)$$

where  $n_v = L_y/L_v$  is the total number of vortices near the N/S interface. The obtained expression for the total conductance (27) consists of two terms. The first term  $G_0 \sim N_0T^2$  coincides with the conductance of the N/S junction at zero magnetic field. The factor  $T^2$  is determined by the probability of the sequential tunneling of the incident and reflected QP through the high interfacial barrier. The second term is the total vortex-induced conductance  $G_{vt} = n_vG_v \sim n_v(k_F\xi)e^{-2K(a)}T$ ; it comes from the tunneling of the incident QP into the zero energy CdGM states inside the vortex core. Indeed it is easy to see that  $e^{-2K(a)}T$ , where  $K(a) = \sqrt{(a/\xi)^2 + 1} - 1$ , is the one-particle tunneling probability through the interfacial barrier and the superconducting layer of the thickness  $a$  with slightly suppressed gap due to the presence of the vortex. The factor  $k_F\xi$  is the number of resonant transverse modes for a single vortex. The vortex-induced conductance  $G_{vt}$  prevails over  $G_0$  when  $a < a_c$ , where the critical distance  $a_c$  is determined by  $a_c \approx (\xi/2)\ln(L_v/T\xi)$ . The parameters of the vortex configuration, such as the intervortex spacing  $L_v$  and the distance  $a$  from the vortex array to the boundary of superconductor are determined by the magnetic field, therefore the conductance of the N/S junction can be controlled by the magnetic field. Using Eq.(2) we obtain that the critical magnetic field  $H_c$  when  $G_{vt} \sim G_0$  is determined by the following transcendental equation  $\ln(x/T) = 2/x$ , where  $x = \sqrt{B/H_{c2}}$ . Taking for example the barrier strength  $Z = 5$ , we obtain that the critical field is  $B_c \sim 0.5H_{c2}$ , and the critical distance  $a_c \sim 1.5\xi$ . Therefore, the influence of the resonant vortex core states on the conductance can become significant when the magnetic field is less than the upper critical and vortices are quite far from the N/S interface.

Finally, we should note that in real N/S junctions the

motion of QP is certainly affected by impurity scattering. The influence of impurities can be neglected completely assuming that the life time of the vortex core states due to the finite barrier transparency is much shorter than the relaxation time of the QP momentum:  $\hbar/\delta E \ll \tau$ , or

$$l_e \gg (Te^{-2a/\xi})^{-1}\xi, \quad (28)$$

where  $l_e = V_F\tau$  is an elastic mean free path of QP at the S region. This condition certainly can be fulfilled if the barrier transparency is not very high, i.e.  $T \sim 1$  and the vortex chain is situated not far from the N/S interface, so that the factor  $Te^{-2a/\xi}$  is not very small. Otherwise, if the condition (28) is not fulfilled, the impurity scattering will modify the conductance. The simplest approach to estimate the conductance in this situation is based on the tunneling hamiltonian, yielding the Eq.(25) for the conductivity. Due to the impurity scattering the local superconducting DOS differs from that given by the Eq.(26), which is valid for the clean case  $l_e \gg \xi$ . In particular, the sharp peak at  $r = 0$  is smeared, therefore at the center of vortex the DOS is smaller as compared to the clean case. But at the distances  $r > \xi$  from the vortex core (e.g. at the N/S interface) the DOS is not suppressed by the impurities even if  $l_e \sim \xi$ . On the contrary, it is even larger than in the clean case due to the smearing of the DOS peak at the center of vortex<sup>21</sup>. Therefore, in case of the rather high impurity concentration on the S side the dependence of the vortex-induced conductance on the magnetic field is still described by the Eq.(2). Another important point is the influence of impurities on the non-resonant part of the conductance, i.e. the first term in Eq.(1). In particular, the interference of QP waves reflected from the interface barrier and impurities on the N side of the N/S junction can also result in the low-bias conductance enhancement, known as reflectionless tunneling (see Ref. 22 and references therein). In experiments where the reflectionless tunneling effect was observed<sup>24</sup> the condition  $l_e > \xi$  was fulfilled. In this case the critical value of magnetic field suppressing the reflectionless tunneling<sup>23</sup>  $H_c \sim \phi_0/(12l_e^2)$  was much less than the upper critical field of the superconductor. In our case the applied magnetic field must be strong enough to create the dense vortex lattice in superconductor:  $B \sim H_{c2} \gg H_c$ . Therefore, under the same experimental conditions as in Ref.24 the reflectionless tunneling effect is absent in the range of magnetic fields that we are interested in.

## VI. CONCLUSION

To summarize, we have investigated the low-energy charge transport in N/S junction across the direction of applied magnetic field. We have found the strong enhancement of the zero-bias conductance due to the resonant tunneling of the incident QP into the subgap vortex core states. The effect is most sound if the conventional channel of Andreev reflection is suppressed by the

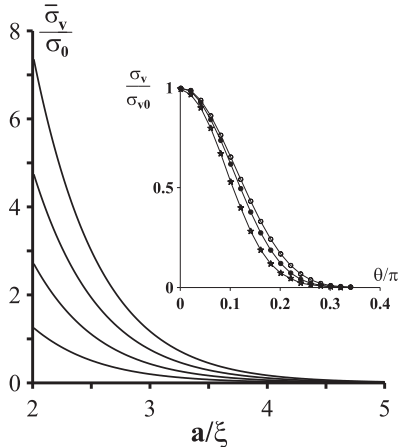


FIG. 2: Plot of the ratio  $\bar{\sigma}_v/\sigma_0$  of the average vortex induced conductivity to the conductivity in the absence of vortices. Curves from top to bottom correspond to  $Z = 5, 4, 3, 2$ . Inset: function  $\sigma_v(\theta)/\sigma_{v0}$  for  $a/\xi = 2$  (open circles),  $a/\xi = 3$  (filled circles)  $a/\xi = 5$  (asterisks);  $Z = 2$ .

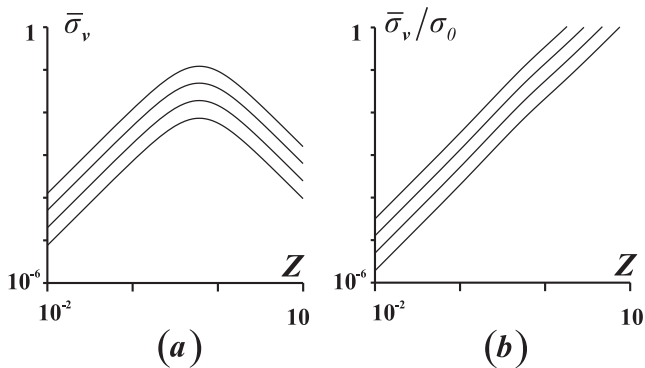


FIG. 3: (a): Plot of the average vortex-induced conductivity  $\bar{\sigma}_v$  as a function of the barrier strength  $Z$  in logarithmic scale. (b): Plot of the ratio  $\bar{\sigma}_v/\sigma_0$  as a function of the barrier strength  $Z$  in logarithmic scale. Curves from top to bottom correspond to  $a/\xi = 2, 2.5, 3, 3.5$ .

high interfacial barrier. Note that usually, the vortex core states are investigated in STS experiments, where the charge transport is measured along the direction of magnetic field. For the alternative to the STS methods now we can suggest the transport measurements in planar structure with wide-area N/S contacts. The vortex induced conductance that we have studied depends exponentially on the distance from the vortex chain to the N/S interface and therefore can be effectively controlled by the external magnetic field. Also for the possible experimental setup one can consider the mesoscopic superconducting sample with lateral tunneling junctions, such as in Ref.2. Since the vortex -induced conductance is proportional to the number of vortices, the conductance vs magnetic field dependence should reveal pronounced steps marking the switch of the total vorticity of the sample.

## VII. ACKNOWLEDGEMENTS

It's my pleasure to thank Dr. Alexander S. Mel'nikov for numerous stimulating discussions and help in preparation of this paper. Also I am grateful to Ekaterina Ezhova for help with numeric calculations. This work was supported, in part, by Russian Foundation for Basic Research, by Program "Quantum Macrophysics" of RAS, and by Russian Science Support and "Dynasty" Foundations.

<sup>1</sup> G. E. Blonder, M. Tinkham and T. M. Klapwijk, Phys. Rev. B **25**, 4515 (1982).

<sup>2</sup> A. Kanda, B. J. Baelus, F. M. Peeters, K. Kadowaki, and Y. Ootuka, Phys. Rev. Lett. **93**, 257002 (2004); B. J. Baelus, A. Kanda, F. M. Peeters, Y. Ootuka and K. Kadowaki, Phys. Rev. B **71**, 140502(R) (2005); B. J. Baelus, A. Kanda, N. Shimizu, K. Tadano, Y. Ootuka, K. Kadowaki, and F. M. Peeters, Phys. Rev. B **73**, 024514 (2006).

<sup>3</sup> G. Boato, G. Gallinaro, and C. Rizzuto, Solid State Commun. **3**, 173 (1965); D. S. McLachlan, Solid State Commun. **8**, 1589 (1970); V. A. Schweigert, F. M. Peeters, and P. S. Deo, Phys. Rev. Lett. **81**, 2783 (1998); A. K. Geim, S. V. Dubonos, J. J. Palacios, I. V. Grigorieva, M. Henini, and J. J. Schermer, Phys. Rev. Lett. **85**, 1528 (2000); L. F. Chibotaru, A. Ceulemans, V. Bruyndoncx, V. V. Moshchalkov, Nature (London) **408**, 833 (2000); A. K.

Geim, S. V. Dubonos, J. J. Palacios, I. V. Grigorieva, M. Henini, and J. J. Schermer, Phys. Rev. Lett. **85**, 1528 (2000).

<sup>4</sup> M. Tinkham, *Introduction to Superconductivity* (McGraw-Hill, New York, 1996), 2nd ed., Chap. 10.

<sup>5</sup> A. Anthore, H. Pothier, and D. Esteve, Phys. Rev. Lett. **90**, 127001 (2003).

<sup>6</sup> C. Caroli, P. G. de Gennes, J. Matricon, Phys. Lett. **9**, 307 (1964).

<sup>7</sup> H. F. Hess, R. B. Robinson, R. C. Dynes, J. M. Valles, Jr., and J. V. Waszczak, Phys. Rev. Lett. **62**, 214 (1989); H. F. Hess, R. B. Robinson, and J. V. Waszczak, Phys. Rev. Lett. **64**, 2711 (1990); A. Kohen, Th. Proslier, T. Cren, Y. Noat, W. Sacks, H. Berger, and D. Roditchev, Phys. Rev. Lett. **97**, 027001 (2006).

<sup>8</sup> C. R. Hu, Phys. Rev. Lett. **72**, 1526 (1994); J. Yang, C. R.

- Hu, Phys. Rev. B **50**, 16766 (1994); Y. Tanaka, S. Kashiwaya, Phys. Rev. Lett. **74**, 3451 (1995); S. Kashiwaya, Y. Tanaka, M. Koyanagi, H. Takashima and K. Kajimura, Phys. Rev. B **51**, 1350 (1995).
- <sup>9</sup> B. Ricco and M. Ya. Azbel, Phys. Rev. B **29**, 1970 (1984)
- <sup>10</sup> J. Bardeen, R. Kummel, A. E. Jacobs and L. Tewordt, Phys. Rev. **187**, 556 (1969)
- <sup>11</sup> N. B. Kopnin, A. S. Melnikov and V. M. Vinokur, Phys. Rev. B **71**, 052505 (2005);
- <sup>12</sup> P. Pincus, Phys. Rev. **158**, 346 (1967);
- <sup>13</sup> J. R. Clem, J. Low Temp. Phys. **18**, 427 (1975)
- <sup>14</sup> G. E. Volovik, Pis'ma Zh. Eksp. Teor. Fiz. **58**, 444 (1993) [JETP Lett. **58**, 455 (1993)].
- <sup>15</sup> F. Gygi and M. Schluter, Phys. Rev. B **43**, 7609 (1991);
- <sup>16</sup> A. S. Mel'nikov, N. B. Kopnin and V. M. Vinokur, Phys. Rev. B **68**, 054528 (2003)
- <sup>17</sup> G. D. Mahan, *Many-particle physics* (Plenum Press, New York, 1993), 2nd ed., Chap. 9.
- <sup>18</sup> S. Graser, C. Iniotakis, T. Dahm and N. Schopohl, Phys. Rev. Lett. **93**, 247001 (2004);
- <sup>19</sup> N. Schopohl and K. Maki, Phys. Rev. B **52**, 490 (1995);
- <sup>20</sup> N. B. Kopnin and G. E. Volovik, JETP Lett. **64**, 690 (1996)
- <sup>21</sup> P. Miranovic, M. Ichioka and K. Machida, Phys. Rev. B **70**, 104510 (2004);
- <sup>22</sup> C.W.J. Beenakker, Rev. Mod. Phys. **69**, 731 (1997);
- <sup>23</sup> B. J. van Wees, P. de Vries, P. Magnee, and T. M. Klapwijk, Phys. Rev. Lett. **69**, 510 (1992);
- <sup>24</sup> A. Kastalsky, A. W. Kleinsasser, L. H. Greene, R. Bhat, F. P. Milliken, and J. P. Harbison, Phys. Rev. Lett. **67**, 3026 (1991)